Neuron, Volume *55*

Supplemental Material

Postsynaptic Positioning of Endocytic Zones and AMPA Receptor Cycling by Physical Coupling of Dynamin-3 to Homer

Jiuyi Lu, Thomas D. Helton, Thomas A. Blanpied, Bence Rácz, Thomas M. Newpher, Richard J. Weinberg, and Michael D. Ehlers

Supplemental Methods

DNA Constructs

The DsRed fusion of the clathrin light chain LCa was provided by Jim Keen and used as described (Gaidarov et al., 1999; Santini et al., 2002). PSD-95-GFP was provided by David Bredt. EGFP tagged dynamin-1aa (*Homo sapiens*), dynamin-2ab (*Rattus norvegicus*) and dynamin-3aaa (*Rattus norvegicus*) were gifts from Mark McNiven. HA-Shank and HA/T-GluR1 cDNA were provided by Morgan Sheng. Dyn1K44A-EGFP, Dyn2K44A-EGFP, and Dyn3K44A-EGFP were generated from wildtype cDNA by site-directed mutagenesis (QuickChange, Stratagene). Dyn1-PRD, Dyn2-PRD, and Dyn3-PRD were amplified by PCR and subcloned into pEGFP-C1 (Clontech) and Flag-CMV2 (gift from Shirish Shenolikar), respectively. Dyn3-ΔPH, Dyn3-ΔGED and Dyn3-Δ819-831 were generated by PCR-based mutagenesis using dynamin3-EGFP as a template. All constructs were verified by DNA sequencing and by immunoblot detection of proteins of the expected molecular mass in HEK 293T cells. GFP-Shank C-tail was amplified by PCR and subcloned into pEGFP-C1 (Clontech). HA-ShankΔPLEF was generated from wildtype HA-Shank by site-directed mutagenesis.

Primary Neuronal Culture and Transfections

Hippocampal neuron cultures were prepared from E18 rat embryos and maintained for 14-24 days *in vitro* as described (Ehlers, 2000). Neurons were transfected with Lipofectamine 2000 (Invitrogen) according to the manufacturer's recommendations, except that 0.5 – 0.7 μg of each DNA construct in 20 μl Opti-MEM and 0.5 μl of Lipofectamine 2000 in 20 μl Opti-MEM were mixed and added to coverslips in 12-well plates.

Live-Cell Imaging

Sixteen to forty-eight hours following transfection, coverslips were imaged at 37°C in a sealed chamber (Dagan) filled with imaging buffer (120 mM NaCl, 3 mM KCl, 2 mM $CaCl_2$, 2 mM $MgCl_2$, 10 mM glucose, 10 mM HEPES, and 2% B27, pH 7.35, 250 mOsm to match culture growth medium). Wide-field epifluorescence images were acquired on a Nikon inverted microscope. Confocal images were obtained using a Yokogawa spinning disk confocal (Solamere Technology Group), with excitation lines from a 2.5W KrAr laser (SpectraPhysics) selected and shuttered via an acousto-optical tunable filter (Neos Technologies) and emission directed through a filter wheel (Sutter Instruments) holding band-pass filters (Chroma). Images were acquired using a 100 × 1.4 NA Plan Apochromat objective and analyzed using Metamorph (Universal Imaging Corporation) with a 12-bit cooled CCD camera (Roper Scientific or Hamamatsu Inc.).

Immunoprecipitation

Forebrains from adult Wistar rats were homogenized, solubilized in lysis buffer (50 mM Tris, 150 mM NaCl, 2 mM EDTA, 2 mM EGTA, 1% Triton X-100, pH 7.4), and cleared by low speed centrifugation (1000 × g, 5 min). Solubilized brain lysates (0.5 mg total protein) were diluted in 0.2 ml lysis buffer and precleared with 50 µl Protein A/G agarose beads (Pierce). Lysates were then incubated with either 15 µg rabbit IgG (Sigma), 5 µl anti-Shank or 5 µl anti-Dyn3 for 4 - 6 hr at 4°C. Immune complexes were precipitated by incubation with 50 µl protein A/G agarose beads for 1 hr followed by centrifugation (2500 rpm, 3 min). Precipitated proteins were washed four times with lysis buffer and one time with lysis buffer without Triton X-100 prior to elution by boiling in 1 × SDS-PAGE sample buffer. Samples were separated by SDS-PAGE, transferred, and subjected to immunoblot analysis as described (Ehlers, 2000).

For dynamin oligomerization assays, HEK 293T cells were transiently transfected with both Flag- and GFP-tagged dynamin constructs using Lipofectamine 2000 (Invitrogen) as instructed by the manufacturer. Cell lysate were prepared by solubilizing transfected cells in lysis buffer (50 mM Tris, 150 mM NaCl, 2 mM EDTA, 2 mM EGTA, 1% Triton X-100, pH 7.4). After preclearing the supernatants with protein A/G beads (Pierce), lysates were then incubated with 2 µg anti-Flag antibody (Sigma) for 4 - 6 hr at 4°C. Immune complexes were

precipitated by incubation with 50 µl protein A/G agarose beads for 1 hr followed by centrifugation (2500 rpm, 3 min). Precipitated proteins were washed four times with lysis buffer and one time with lysis buffer without Triton X-100 prior to elution by boiling in 1 × SDS-PAGE sample buffer. Samples were separated by SDS-PAGE, transferred to a PVDF membrane, and subjected to immunoblot analysis.

Immunocytochemistry, Trafficking Assays and Antibodies

Cultured hippocampal neurons were fixed for 10 min in prewarmed PBS with 2 mM Ca^{2+} containing 4% paraformaldehyde/4% sucrose and then permeabilized with 0.2% Triton X-100 in PBS. Neurons were incubated with mouse anti-VGLUT1 (Synaptic Systems, 1:1000), or rabbit anti-Dyn3 (a gift from Mark McNiven, 1:400) overnight at 4°C. Cells were washed and incubated with Alexa 647-conjugated secondary antibody (Molecular Probes) for 1 hr at room temperature.

Endogenous surface AMPA receptor staining. Live hippocampal neurons were incubated with rabbit anti-GluR1 N-terminal antibody (O'Brien et al., 1998; Ehlers, 2000) for 20 min at 10°C to label surface AMPA receptors. After washing, neurons were fixed with 4% paraformaldehyde/4% sucrose. Cells were washed and incubated with Alexa 568-conjugated secondary antibodies (Molecular Probes) for 1 hr at room temperature.

NMDA receptor-only synapses. After endogenous surface AMPA receptor labeling by rabbit anti-GluR1 N-terminal antibody (O'Brien et al., 1998; Ehlers, 2000), cells were fixed and permeabilized with methanol followed by 0.2% Triton X-100 in PBS. Neurons were then incubated with mouse anti-NR1 (Affinity Bioreagents, 1:1000) overnight at 4°C prior to incubation with Alexa 568- and Alexa 647-conjugated secondary antibodies.

AMPA receptor endocytosis assay. Neurons were pre-treated for 1 hr with 100 µg/ml of the lysosomal protease inhibitor leupeptin before antibody feeding. Endogenous GluR1 was labeled live with rabbit anti-GluR1 N-terminal antibody (O'Brien et al., 1998; Ehlers, 2000) for 20 min at 10°C and internalization enabled for 5, 20, 30 min by switching to 37°C. After fixation, surface-remaining GluR1 was blocked with unlabeled rabbit secondary antibody (Johnson & Johnson Immunology) for 5 hr at room temperature. Cells were then permeabilized with 0.2% Triton X-100, and incubated with Cy3-conjugated secondary antibody for 1 hr at room temperature. To measure surface GluR1 levels, cells were labeled live with anti-GluR1

antibody, fixed and incubated with Cy3-conjugated secondary antibody for 1 hr at room temperature. As a blocking control, cells were fixed after anti-GluR1 live labeling and incubated with unlabeled rabbit secondary antibody for 5 hr at room temperature. Cells were then incubated with Cy3-conjugated secondary antibody for 1 hr at room temperature (Supplementary Figure S10A).

AMPA receptor recycling assay. Neurons were co-transfected with HA/T-GluR1 and either GFP, Dyn3-PRD or Dyn3-P800L for 6 days (14-20 DIV). Surface HA/T-GluR1 was labeled by incubating live neurons with mouse anti-HA (2 μg/ml; Covance) for 20 min at 10°C and receptor-antibody complexes internalized for 30 min at 37°C. Remaining surface HA/T-GluR1 was blocked with unlabeled mouse secondary antibody (Sigma). Neurons were then incubated for 1 hr at 37°C to allow recycling of internalized receptors. After fixation, neurons were incubated with Cy3-conjugated secondary antibody to label recycled AMPA receptors on the cell surface. Cells were then permeabilized with 0.2% Triton X-100 and incubated with mouse anti-VGLUT1 overnight at 4°C prior to washing and incubation with Alexa 647-conjugated secondary antibody for 1 hr at room temperature. For blocking controls, cells were kept at 10°C for 1 hr after internalization (Supplemental Figure S10B).

Transferrin endocytosis assay. Neurons were serum starved in Neurobasal media for 15 min, and then incubated with Alexa 568-Tf (50 μg/ml) for 20 min at 10°C and internalization allowed for 5, 10, 15 or 20 min at 37°C in the presence of unlabeled Tf (5 mg/ml). Remaining surface-bound transferrin was then acid-stripped (PBS, pH 5.0) on ice. After washing, neurons were fixed and intracellular Alex 568-Tf was imaged. For measuring surface transferrin levels, cells were fixed and imaged after Alexa 568-Tf labeling without moving to 37°C.

Transferrin recycling assay. Neurons were incubated with Alexa 568-Tf (50 μg/ml) in serum-free Neurobasal media for 1 hr at 37°C to reach equilibrium. Neurons were then treated with an excess unlabeled Tf (5 mg/ml) for 25 min at room temperature. After washing, neurons were fixed and the remaining intracellular Alexa 568-Tf was imaged. Loss of Alexa-Tf reflects recycling.

Image Analysis and Quantification

For fixed samples, images were acquired with a Leica TCS SP2 laser scanning confocal microscope and analyzed using Metamorph (Universal Imaging Corporation). To measure the

average pixel fluorescence intensity, neurons were carefully traced and the background intensity subtracted from the intensity in the traced regions. Neurons were selected blind based on GFP fluorescence. Unless otherwise indicated, n values correspond to the number of neurons analyzed from two to five independent experiments. For EZ-negative synapse analysis, circular regions with a diameter of 0.7 μm were selected based on PSD-95 or VGLUT1 puncta. All the regions were transferred to the clathrin-DsRed channel. The percentage of EZ negative synapse was calculated by 100 × [1- (the number of PSD95 or VGLUT puncta containing clathrin puncta/the number of total PSD-95 or VGLUT1 puncta)]. For NMDA receptor-only synapse analysis, the percentage of NMDA receptor-only synapses was calculated by the following formula: 100 × [1- (the number of NMDA receptor puncta containing AMPA receptor puncta/the number of total NMDA receptor puncta)]. The n values indicated correspond to the number of neurons analyzed.

Electron Microscopy

Immunocytochemistry for pre-embedding electron microscopy. Deeply anesthetized male Sprague-Dawley rats (200-350 g) were perfused with saline followed by ice-cold fixative, containing 4% paraformaldehyde, 0.2% glutaraldehyde in 0.1 M phosphate buffer (PB, pH 7.4). Brains were removed and postfixed in 4% paraformaldehyde for 2 h. Coronal sections (50 μm thick) were cut with a Vibratome, then washed in PB; free-floating sections were treated with $NaBH_4$, blocked with normal donkey serum (NDS, 10%) in phosphate-buffered saline (PBS, pH 7.4), followed by incubations in the primary and secondary antibodies. Rabbit pan-Dyn3 antibody was diluted in PBS containing 2% NDS. Following rinses in PBS, sections were incubated in biotinylated anti-rabbit IgG (Jackson, USA) for 2 h and then streptavidin coupled to 1.4 nm gold particles (1:80, Nanoprobes Inc.) for 3 h, and rinsed in PBS. Sections were washed in 0.1 M sodium acetate (to remove phosphate and chloride ions), followed by silver enhancement with IntenS EM kit (Amersham Biosciences). Sections were then postfixed with 0.5% OsO_4, contrasted in 1% uranyl acetate in maleate buffer, dehydrated and embedded with epoxy resin (Epon/Spurr's; EMS). No specific immunoreactivity could be detected when either the primary or the secondary antibody was omitted prior to silver enhancement. For electron microscopy, ~70 nm thin sections were cut on a Reichert ultramicrotome, mounted on 200 mesh copper grids, contrasted with uranyl acetate and Sato's lead, then examined in a Philips Tecnai

electron microscope at 80 kV. Digital micrographs were acquired with a Gatan 12 bit 1024 × 1024 CCD camera. Contrast, density, and sharpness of final images for plates were adjusted using Adobe Photoshop CS.

Quantitative analysis of immunogold labeling. Tangential distribution of dynamin-3 immunogold labeling was measured according to Racz et al (2004). Briefly, electron micrographs were taken from single ultrathin sections from randomly selected fields in stratum radiatum of the hippocampal CA1 region that included at least one immunolabeled spine with an identifiable PSD. Micrographs were analyzed with ImageJ v.1.29 software. Gold particles were considered to be associated with the plasma membrane ("shell") if they were within 60 nm of the extracellular side of the membrane (a distance reflecting antibody size + particle size + membrane thickness). To permit pooling of data, distances were normalized according to the equation:

$$d_N = 1 - \frac{|d_1 - d_2|}{d_1 + d_2}$$

For each immunopositive spine, we measured the distances of the center of the gold particles from the closer (d_1) and farther (d_2) edges of the PSD along the plasma membrane; to compute spine circumference, we also measured the length of the PSD. Thus, a gold particle adjacent to the PSD edge would have a value of 0, whereas 1 would correspond to a particle lying on the membrane equidistant between the two edges of the PSD (see Figure 3B inset for explanation). We performed our analysis after eliminating sparse particles lying within the PSD (since the pre-embedding method used here does not permit reliable quantification of antigen within the PSD).

Electrophysiology

Whole-cell voltage clamp recordings were performed on DIV 17-24 hippocampal neurons cultured at high density on poly-lysine coated glass coverslips. Transfection efficiencies were typically <1% and autapses are rare in our cultures, ensuring that any observed effect of expressing dynamin-3 constructs originates in the postsynaptic neuron. Neurons were held at –60 mV using a MultiClamp 700A amplifier (Axon Instruments, Foster City, CA) controlled with a Pentium PC running MultiClamp Commander and pClamp (Axon Instruments). The extracellular solution contained (in mM): 150 NaCl, 5 KCl, 10 HEPES, 1 $MgCl_2$, 30 D-glucose, 2 $CaCl_2$, 0.001 TTX, 0.03 bicuculline (330 mOsm/l, pH 7.4). Recording pipettes, with

resistances between 3-5 MΩ, were filled with a solution containing (in mM): 30 $CsSO_4$, 70 K_2SO_4, 25 HEPES, 25 N-methyl-D-glucamine, 0.1 $CaCl_2$, 1 EGTA, 2 Na_2ATP, 0.1 leupeptin (300 mOsm/l, pH 7.2). Data were analyzed using MiniAnalysis software (Synaptosoft, Decatur, GA). Detection criteria for mEPSC included amplitude greater than 5 pA and rise times from the onset to the peak of less than 5 msec.

RNA interference

Two separate DNA oligonucleotides containing a 29 or 19 nucleotide sequence specific to the rat dynamin-3 gene, a 10 nucleotide loop region (TTGATATCCG), and the 29 or 19 nucleotide antisense dynamin-3 sequence were annealed to their antisense counterparts and ligated into the pRNAT-H1.3-Hygro plasmid (Genscript) downstream of the H1.3 promoter. These shRNA constructs were transfected in cultured hippocampal neurons for 6 days *in vitro* using Lipofectamine 2000 (Invitrogen). The target shRNA sequences were: *d3RNAi-2* (29mer), GGATCCCGTCGCCAATGATCGCGAGGGCTTCTTTCATTGATATCCGTGAAAGAAGCC CTCGCGATCATTGGCGACTTTTTTCCAAAAGCTT; and *d3RNAi-4* (19mer), GGATCCCATGCGATTGATCTTAGCACTTGATATCCGGTGCTAAGATCAATCGCATTT TTTTCCAAAAGCTT, respectively. For dynamin-2, the target shRNA sequence, *d2RNAi-2*, was AGGACAUGAUCCUGCAGUUUAUCAGCCGGCCAACCGGCUGAUAAACUGCAGGAUC AUGUCCUUU. As a negative control, a scrambled shRNA construct was made in the same manner as above. The sequence was GGATCCCGCCATTCTGAATCGGTAAGCGACCAATCGCTTACCGATTCAGAATGGTTT TTTCCAAAAGCTT.

Phalloidin Staining

Cultured hippocampal neurons (DIV 14-20) expressing corresponding constructs were fixed for 10 min in prewarmed PBS with 2 mM Ca^{2+} containing 4% paraformaldehyde/4% sucrose and then incubated with phalloidin-Alexa 594 (1:500, Molecular Probes) for 1 hr at room temperature.

Fluorescence Recovery after Photobleaching (FRAP)

Hippocampal neurons were transfected with EGFP-actin together either empty vector, Flag-Dyn3, or Flag-Dyn3-P800L. Live cell imaging was performed at 37°C on a Zeiss LIVE Duoscan confocal microscope. Images were captured every 1 s during a 100 s time course. Regions of interest (ROIs) were bleached between the third and fourth frame using 5 iterations and 100% power from the 489 nm laser line. After background subtraction, the mean pixel intensity of the bleached and unbleached ROIs were divided by their prebleach intensity to give the percent initial intensity. To correct for photobleaching, the percent initial fluorescence of the bleached ROI was divided by the unbleached ROI to give the normalized intensity. The τ of fluorescent recovery was determined by fitting recovery data to a single exponential function of the form $y = y_0 + A(1-e^{(-kx)})$ generated by Origin 7.5.

References

Ehlers, M. D. (2000). Reinsertion or degradation of AMPA receptors determined by activity-dependent endocytic sorting. Neuron *28*, 511-525.

Gaidarov, I., Santini, F., Warren, R. A., and Keen, J. H. (1999). Spatial control of coated-pit dynamics in living cells. Nat Cell Biol *1*, 1-7.

O'Brien, R. J., Kamboj, S., Ehlers, M. D., Rosen, K. R., Fischbach, G. D., and Huganir, R. L. (1998). Activity-dependent modulation of synaptic AMPA receptor accumulation. Neuron *21*, 1067-1078.

Santini, F., Gaidarov, I., and Keen, J. H. (2002). G protein-coupled receptor/arrestin3 modulation of the endocytic machinery. J Cell Biol *156*, 665-676.

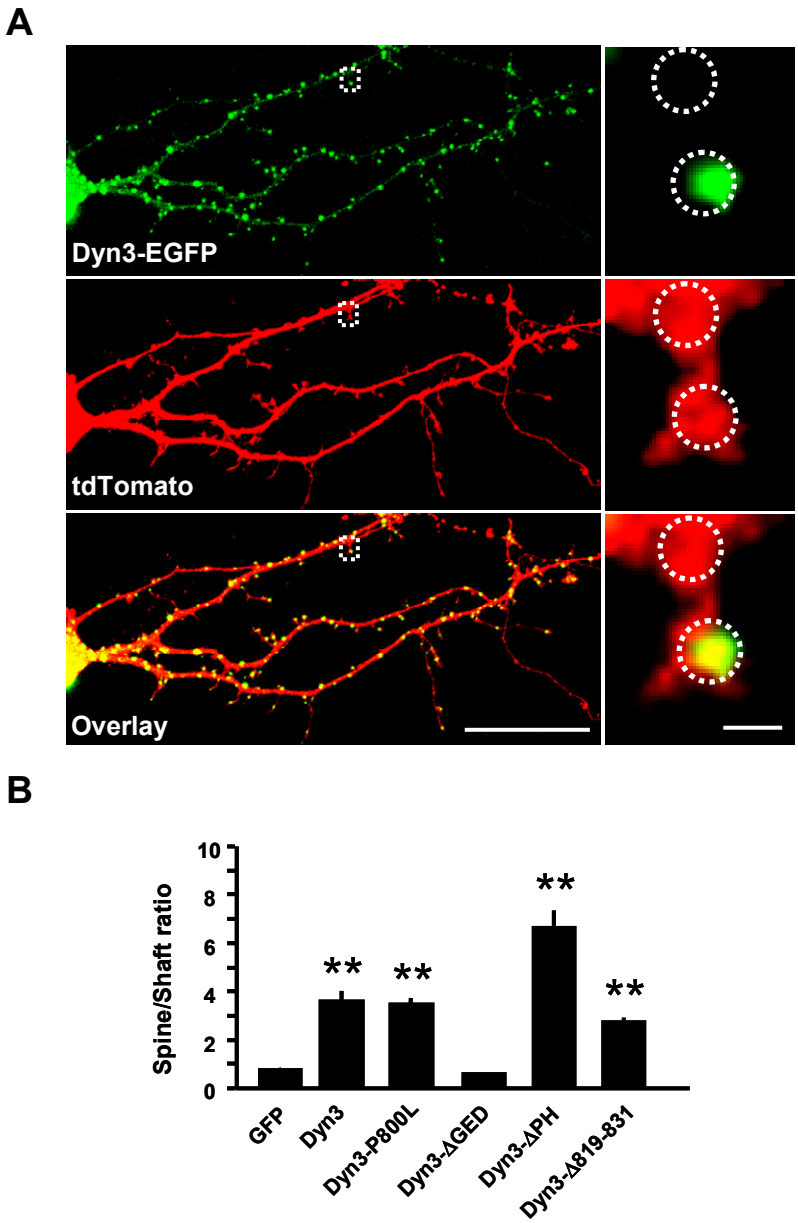

Supplementary Figure S1. Molecular Determinants of Dynamin-3 Spine Targeting
(A) Spine localization of postsynaptically expressed GFP-Dyn3 (green) in a hippocampal neuron (DIV 14-20) expressing tdTomato as a cell fill. Right panels correspond to regions in the dashed white boxes. Scale bars, 30 μm and 1 μm. White dashed circles on the right panels indicate regions selected for spine and shaft intensity measurement.
(B) Quantification of spine enrichment. Hippocampal neurons (DIV 14-20) were transfected with either GFP or with wildtype or mutant forms of dynamin-3-EGFP. Spine targeting was quantified by the ratio of fluorescent intensities in spines relative to the dendritic shaft. Unequivocal assignment of postsynaptic localization of expressed proteins was ensured by low efficiency transfection in high density cultures. Spine/shaft ratio, GFP, 0.78 ± 0.05, n = 5, 125 spines; Dyn3, 3.7 ± 0.4, n = 3, 40 spines; Dyn3-P800L, 3.6 ± 0.3, n = 5, 114 spines; Dyn3-ΔGED, 0.63 ± 0.03, n = 9, 141 spines; Dyn3-ΔPH, 6.69 ± 0.61, n = 10 neurons, 202 spines; Dyn3-Δ819-831, 2.76 ± 0.12, n = 6 neurons, 232 spines; ** $p < 0.001$ relative to GFP control, t-test.

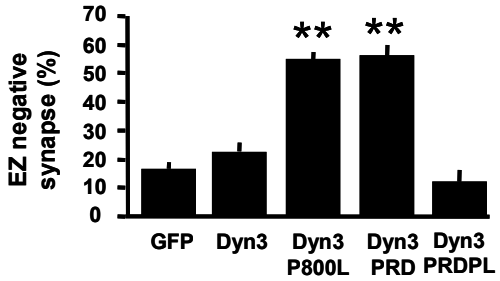

Supplementary Figure S2. Dynamin-3 Positions the EZ at VGLUT-Positive Synapses by Binding Homer

Hippocampal neurons co-expressing clathrin-DsRed with either GFP or GFP-tagged Dyn3, Dyn3-PRD, Dyn3-P800L, or Dyn3-PRDPL were fixed and excitatory synapses visualized by staining for VGLUT1. Data indicate means ± SEM of the fraction of VGLUT-positive puncta lacking postsynaptically associated clathrin-DsRed (EZ negative synapses). GFP, 15.2 ± 0.7%, n = 70; Dyn3wt, 18.9 ± 2.6%, n = 14; Dyn3-P800L, 54.8 ± 2.6%, n = 15; Dyn3-PRD, 56.2 ± 3.5%, n = 17; Dyn3-PRDPL, 11.0 ± 1.3%, n = 11; ** $p < 0.001$ relative to GFP control; t-test. Note that expression of either the proline-rich domain (PRD) of dynamin-3 (Dyn3-PRD) or full-length dynamin-3 that cannot bind Homer (Dyn3-P800L) significantly increased the fraction of synapses lacking an endocytic zone (EZ). Introduction of the P800L mutation into Dyn3-PRD (Dyn3-PRDPL) rendered it unable to disrupt spine EZ localization.

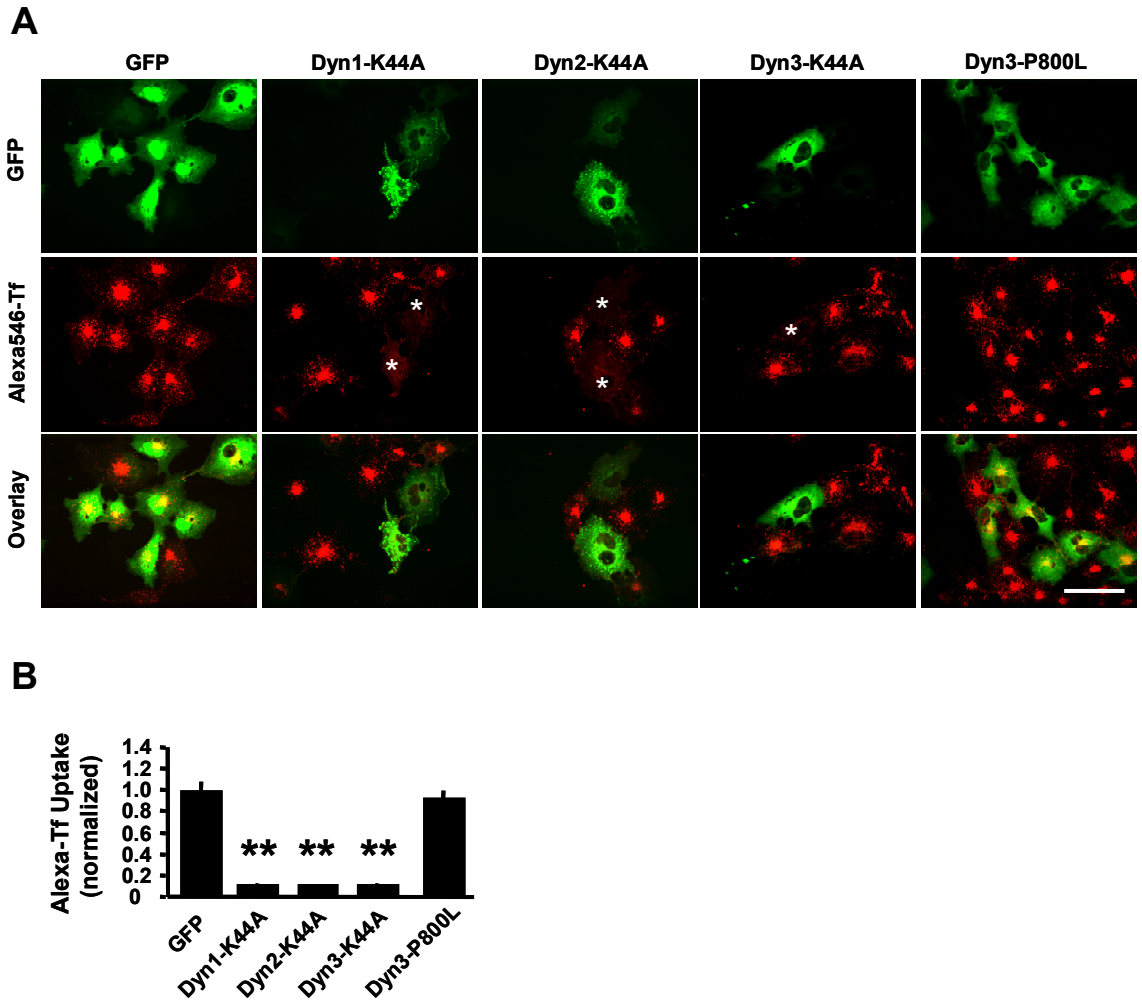

Supplementary Figure S3. GTPase Activity but Not Homer Binding is Required for Endocytosis Mediated by Dynamin-3

(A) GTPase-deficient dynamins (K44A) inhibit transferrin (Tf) endocytosis. Images are maximal projections of confocal stacks showing Alexa 546-Tf uptake in COS7 cells expressing the indicated constructs. Asterisks indicate transfected cells. Scale bar, 50 μm.

(B) Quantification of Tf uptake. Data represent means ± SEM. Normalized internalized Tf fluorescence: GFP, 1.00 ± 0.09, n = 32; Dyn1-K44A, 0.11 ± 0.01, n = 23; Dyn2-K44A, 0.11 ± 0.01, n = 33; Dyn3-K44A, 0.11 ± 0.01, n = 17; Dyn3-P800L, 0.89 ± 0.06, n = 32; ** $p < 0.001$ relative to GFP; t-test.

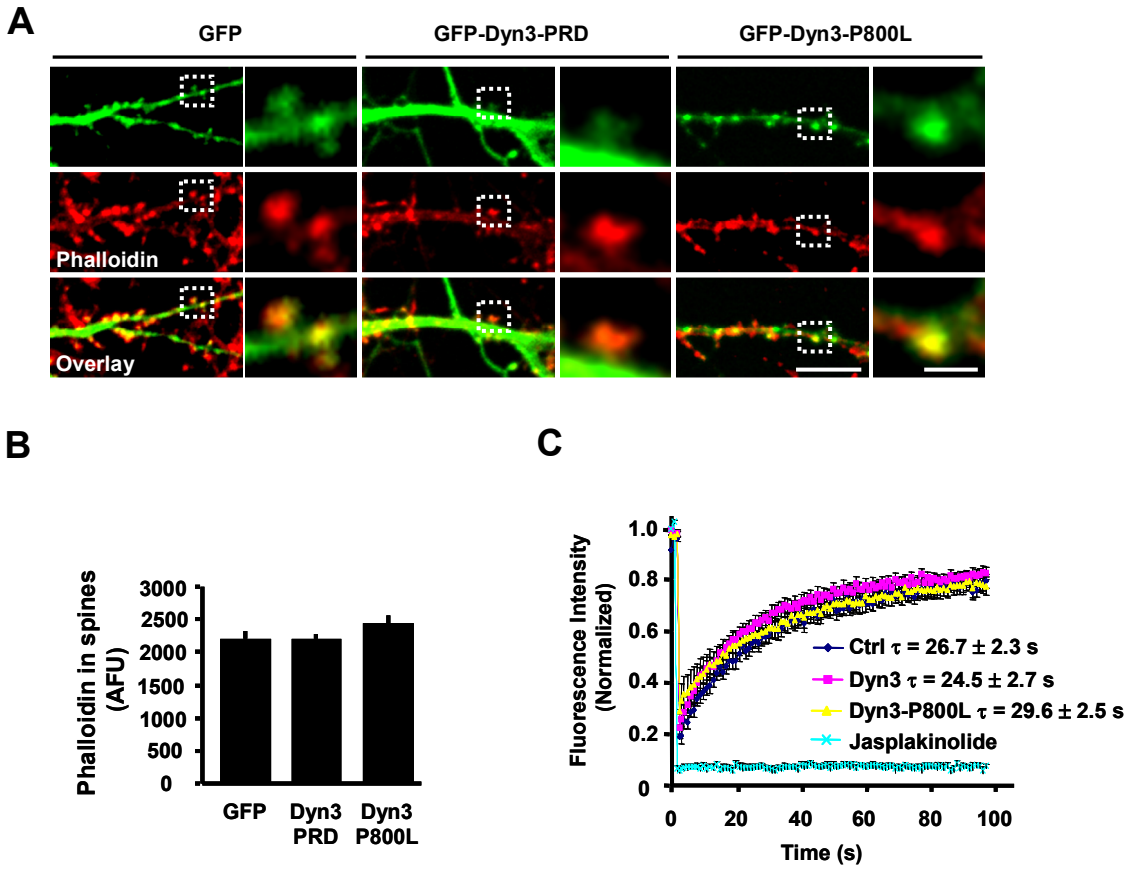

Supplementary Figure S4. Mislocalizing the EZ Does Not Alter Spine Actin
(A) Disruption of dynamin-3 does not affect F-actin content in spines. Actin filaments were visualized by phalloidin-Alexa 594 labeling of hippocampal neurons expressing either GFP, Dyn3-PRD or Dyn3-P800L. Right panels correspond to regions in the dashed white boxes. Scale bars, 10 μm and 1 μm.
(B) Quantification of phalloidin intensity in spines. Average intensity in spines, AFU: GFP, 2192 ± 125, n = 71 spines; Dyn3-PRD, 2190 ± 70, n = 159 spines; Dyn3-P800L, 2427 ± 125, n = 108 spines; $p > 0.05$ relative to control; t-test.
(C) Quantification of actin turnover rate in spines. Hippocampal neurons were transfected with GFP-actin and either Flag empty vector, Flag-Dyn3 or Flag-Dyn3-P800L. GFP-actin in dendritic spines was photobleached and fluorescence recovery after photobleaching (FRAP) monitored over time as a measure of actin exchange kinetics. Note that the exchange rate of actin is unaltered by expression of Dyn3 or Dyn3-P800L, but can be completely inhibited by the actin-stabilizing agent jasplakinolide (10 μM). Time constants (τ) determined by single exponential fits are shown. Empty vector, $\tau = 26.7 \pm 2.3$ s, n = 9 neurons, 16 spines; Flag-Dyn3, $\tau = 24.5 \pm 2.7$ s, n = 9 neurons, 21 spines; Flag-Dyn3-P800L, $\tau = 29.6 \pm 2.5$ s, n = 10 neurons, 29 spines; $p > 0.05$ relative to control, t-test.

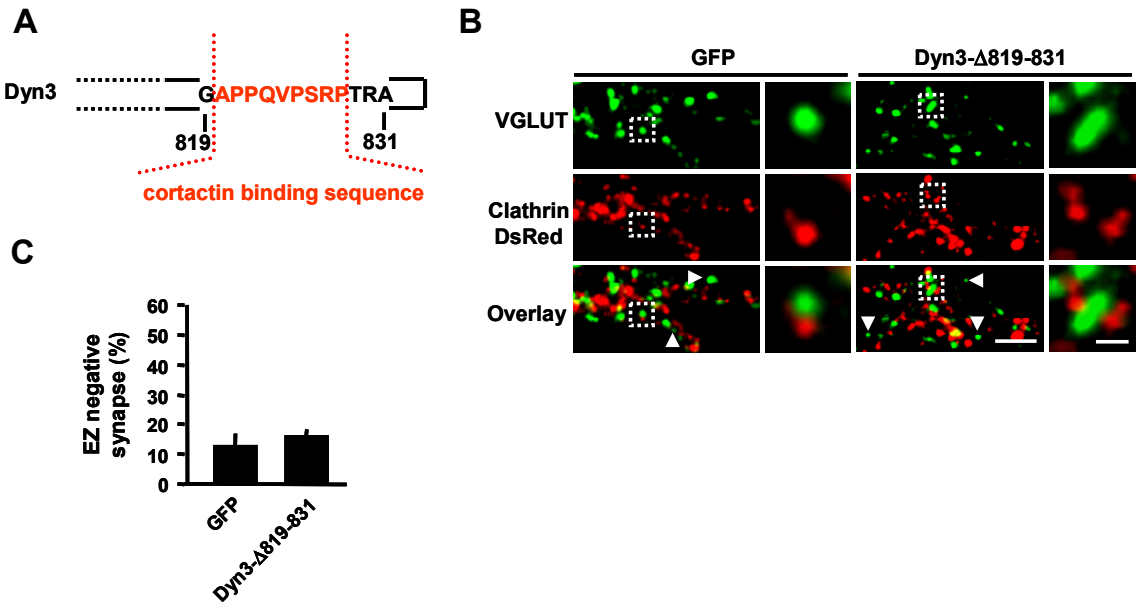

Supplementary Figure S5. Dyn3-Dependent Positioning of the Spine EZ is Independent of Cortactin Binding

(A) Schematic diagram of the cortactin-binding motif within the proline rich domain of dynamin-3 (Dyn3).

(B) Postsynaptic expression of cortactin-binding-deficient dynamin-3 does not alter EZ localization. Images are of hippocampal neurons expressing either GFP or GFP-Dyn3-Δ819-831 together with clathrin-DsRed. Cells were fixed and stained for the excitatory synapse marker VGLUT1. Right panels correspond to regions in the dashed white boxes. Scale bars, 5 μm and 1 μm. Arrowheads indicate clathrin-negative synapses.

(C) Quantification of endocytic zone (EZ)-negative synapses in neurons expressing cortactin-binding-deficient dynamin-3 (Dyn3-Δ819-831) or GFP control. Deletion of the cortactin-binding domain has no effect on EZ positioning next to the PSD. Percent of EZ-negative synapses: GFP, 13.3 ± 2.3 %; Dyn3-Δ819-831, 16.0 ± 1.2 %; n = 14, 10; $p > 0.05$ relative to control, t-test.

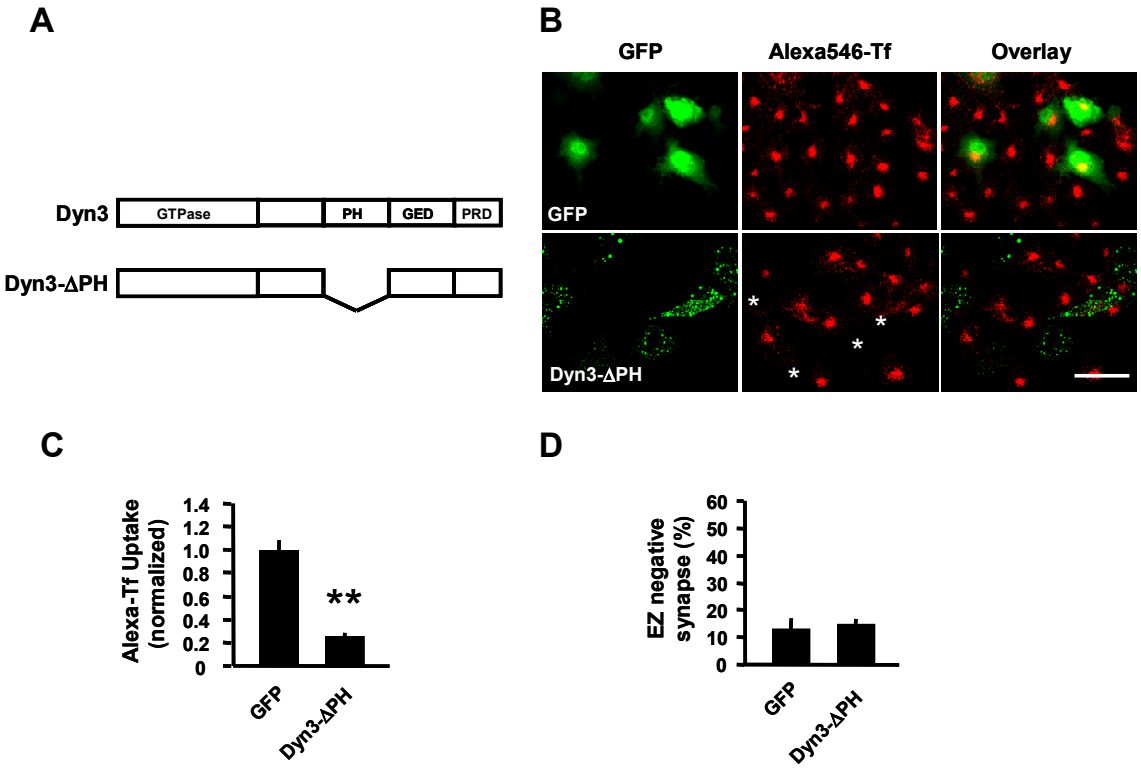

Supplementary Figure S6. Deletion of the Dynamin-3 PH Domain Disrupts Endocytosis but Does Not Affect EZ Localization

(A) Schematic diagram of wildtype dynamin-3 and a deletion mutant lacking the pleckstrin homology (PH) domain (Dyn3-ΔPH).

(B) Expression of GFP-Dyn3-ΔPH inhibits Tf uptake in COS7 cells. Asterisks indicate transfected cells. Scale bar, 50 μm.

(C) Quantification of internalized Tf fluorescence. Data represent means ± SEM. Normalized internalized Tf fluorescence: GFP, 1.00 ± 0.05; Dyn3-ΔPH, 0.25 ± .0.3; n = 32, 63; ** $p < 0.001$ relative to control, t-test.

(D) Disupting dynamin-3 phosphoinositide binding does not affect EZ positioning near the PSD. Data represent means ± SEM of the percent EZ-negative synapses. GFP, 13.3 ± 2.3 %, n = 14; Dyn3-ΔPH, 15.7 ± 1.7 %, n = 8; $p > 0.05$ relative to control, t-test.

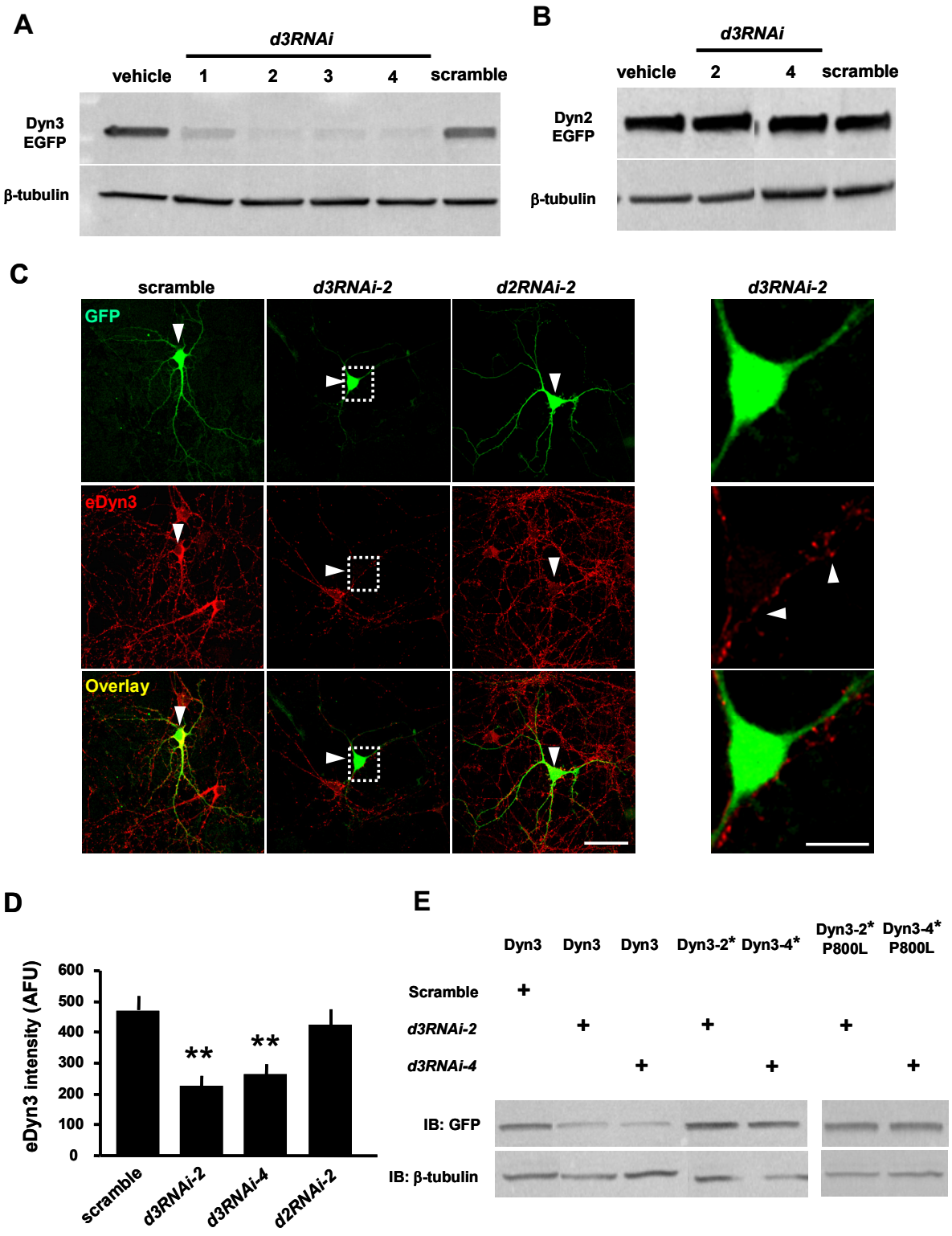
A
d3RNAi
vehicle
1
2
3
4
scramble
Dyn3 EGFP
β-tubulin
B
d3RNAi
vehicle
2
4
scramble
Dyn2 EGFP
β-tubulin
C
scramble
d3RNAi-2
d2RNAi-2
d3RNAi-2
GFP
eDyn3
Overlay
D
eDyn3 intensity (AFU)
600
500
400
300
200
100
0
**
**
scramble
d3RNAi-2
d3RNAi-4
d2RNAi-2
E
Dyn3
Dyn3
Dyn3
Dyn3-2*
Dyn3-4*
Dyn3-2* P800L
Dyn3-4* P800L
Scramble
d3RNAi-2
d3RNAi-4
IB: GFP
IB: β-tubulin

Supplementary Figure S7. Knock-Down of Dynamin-3 by RNA Interference
(A) HEK 293T cells were co-transfected with EGFP-Dyn3 and either siRNA duplexes targeting dynamin-3 (*d3RNAi*) or a scrambled siRNA control. Cells were lysed three days later and dynamin-3 expression level was detected by immunoblot using an anti-GFP antibody. Endogenous β-tubulin was used as an expression control.
(B) Dynamin-3 targeted RNAi sequences specifically knock down dynamin-3 and not dynamin-2 (Dyn2). HEK 293T cells were co-transfected with EGFP-Dyn2 and siRNA duplexes as in (A). Dyn2 expression level was detected by anti-GFP immunoblot. Endogenous β-tubulin was used as an expression control.
(C) Knock-down of endogenous dynamin-3 (eDyn3) expression by RNA interference. Hippocampal neurons were transfected with bicistronic plasmids expressing either *d3RNAi-2* to target dynamin-3, *d2RNAi-2* to target dynamin-2, or a scrambled shRNA control along with GFP (arrowheads). Endogenous dynamin-3 was detected by immunostaining. Note that expression of *d3RNAi-2* but not *d2RNAi-2* reduces eDyn3 levels. Right panels correspond to regions in the dashed white boxes. The remaining staining onto the transfected cells largely reflects presynaptic dynamin-3 from non-transfected axons (arrowheads). Scale bars, 50 μm, 15 μm.
(D) Data represent means ± SEM of endogenous dynamin-3 (eDyn3) fluorescence intensity on neurons expressing the indicated shRNA vectors targeting dynamin-3 (*d3RNAi*) or dynamin-2 (*d2RNAi*). n values are 9, 14, 14, and 11, respectively, ** $p < 0.001$ relative to scrambled shRNA control, t-test. AFU, arbitrary fluorescence units.
(E) Generation of RNAi resistant dynamin-3 cDNAs. HEK 293T cells were transfected with plasmids expressing either *d3RNAi-2*, *d3RNAi-4*, or a scrambled shRNA control together with cDNAs encoding GFP-tagged wildtype dynamin-3 (Dyn3) or GFP-tagged dynamin-3 containing silent third site codon mutations (Dyn3-2*, Dyn3-4*) to produce mismatches with *d3RNAi-2* and *d3RNAi-4*, respectively. Dyn3 expression level was detected by anti-GFP immunoblot (IB). Endogenous β-tubulin was used as an expression control.

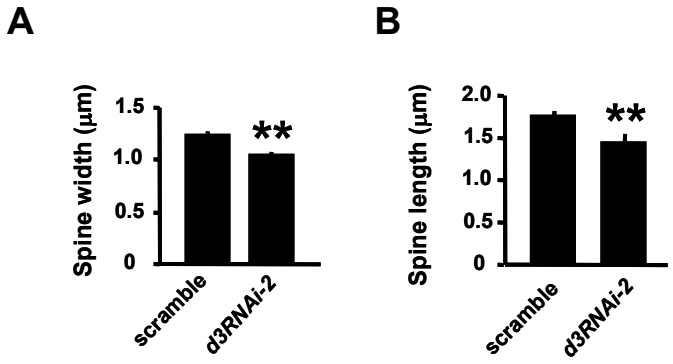

Supplementary Figure S8. Knock-Down of Dynamin-3 Causes a Small Decrease in Spine Size **(A)** and **(B)** Quantifications of spine width (A) and length (B) in hippocampal neurons expressing shRNAs against dynamin-3 (DIV 6–14). Spine width, scrambled, 1.24 ± 0.02 μm, 118 spines; *d3RNAi-2*, 1.04 ± 0.03 μm, 111 spines; spine length, scrambled, 1.76 ± 0.03 μm; *d3RNAi-2*, 1.44 ± 0.06; ** $p < 0.01$ relative to control, t-test.

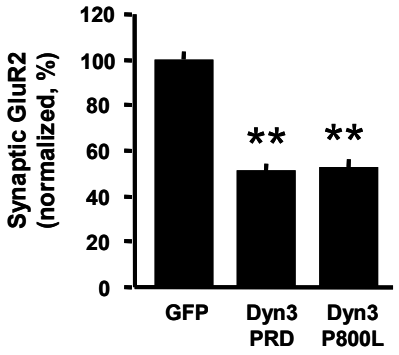

Supplementary Figure S9. Disruption of the EZ Causes Loss of Synaptic GluR2
Data represent means ± SEM of surface synaptic GluR2 fluorescence intensity at synapses of hippocampal neurons expressing the indicated constructs. n = 10, 19 and 14, ** $p < 0.001$ relative to GFP, t-test.

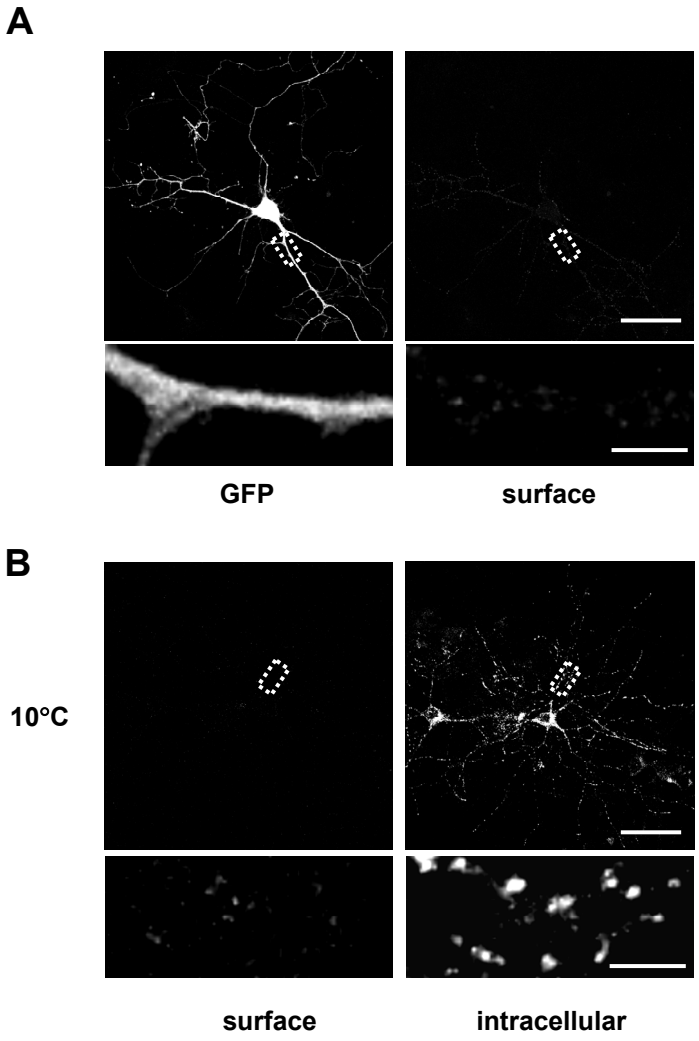

Supplementary Figure S10. Controls for GluR1 Endocytosis and Recycling Assays
(A) In the absence of 37°C incubation, surface GluR1 is completely blocked by excess unlabeled secondary antibody. Hippocampal neurons expressing GFP (14-20 DIV) were incubated live with an anti-GluR1 N-terminal antibody at 10°C for 20 min. After fixation, surface-labeled GluR1 was blocked by incubation with unlabeled IgG prior to incubation with Alexa-568 labeled secondary antibody (right panel). Surface-labeled GluR1 was completely blocked under these conditions.
(B) Blocking control for GluR1 recycling assays. Hippocampal neurons (14-20 DIV) expressing HA-GluR1 were incubated live with an anti-HA antibody at 10°C for 20 min, then incubated at 37°C for 30 min to allow endocytosis. Remaining surface HA-GluR1 was blocked with unlabeled mouse secondary antibody and neurons were then incubated for 1 hr at 10°C to inhibit receptor recycling. After fixation, neurons were incubated with Alexa 568-conjugated secondary antibody to label remaining unblocked AMPA receptors on the surface (left panel), followed by permeabilization and labeling for intracellular HA-GluR1 (right panel). Note that 10°C incubation prevented GluR1 recycling and surface-labeled HA-GluR1 was almost completely blocked under these conditions.